



Preparation, crystal structure, and spectroscopic, chemical, and electrochemical properties of (2*E*,4*E*)-4-[4-(dimethylamino)phenyl]-1-(3-guaiazulenyl)-1,3-butadiene compared with those of (*E*)-2-[4-(dimethylamino)phenyl]-1-(3-guaiazulenyl)ethylene

Shin-ichi Takekuma^{a,*}, Hiroto Matsuoka^a, Toshie Minematsu^b, Hideko Takekuma^a

^a Department of Applied Chemistry, Faculty of Science and Engineering, Kinki University, 3-4-1 Kowakae, Higashi-Osaka-shi, Osaka 577-8502, Japan

^b School of Pharmaceutical Sciences, Kinki University, 3-4-1 Kowakae, Higashi-Osaka-shi, Osaka 577-8502, Japan

ARTICLE INFO

Article history:

Received 3 December 2009

Received in revised form 16 February 2010

Accepted 17 February 2010

Available online 21 February 2010

Keywords:

(2*E*,4*E*)-1,3-Butadiene derivative

Crystal structures

Diels–Alder adducts

Extended π -electron system

Guaiazulene

Properties

Wittig reaction

ABSTRACT

Wittig reaction of 3-[4-(dimethylamino)phenyl]propanal (**5**) with (3-guaiazulenylmethyl)triphenylphosphonium bromide (**4**) in ethanol containing NaOEt at 25 °C for 24 h under argon gives the title (2*E*,4*E*)-1,3-butadiene derivative **6E** in 19% isolated yield. Spectroscopic properties, crystal structure, and electrochemical behavior of the obtained new extended π -electron system **6E**, compared with those of the previously reported (*E*)-2-[4-(dimethylamino)phenyl]-1-(3-guaiazulenyl)ethylene (**12**), are documented. Furthermore, reaction of **6E** with 1,1,2,2-tetracyanoethylene (TCNE) in benzene at 25 °C for 24 h under argon affords a new Diels–Alder adduct **8** in 59% isolated yield. Along with spectroscopic properties of the $[\pi 4 + \pi 2]$ cycloaddition product **8**, the crystal structure, possessing a *cis*-3,6-substituted 1,1,2,2-tetracyano-4-cyclohexene unit, is shown. Moreover, reaction of **6E** with (*E*)-1,2-dicyanoethylene (DCNE) under the same reaction conditions as the above gives no product; however, this reaction in *p*-xylene at reflux temperature (138 °C) for four days under argon affords a new Diels–Alder adduct **9** in 54% isolated yield. Although reaction of **6E** with DCNE in toluene at reflux temperature (110 °C) for four days under argon provides **9** very slightly, reaction of **6E** with dimethyl acetylenedicarboxylate (DMAD) in toluene at reflux temperature for two days under argon yields a new Diels–Alder adduct **10**, in 58% isolated yield, which upon oxidation with MnO₂ in CH₂Cl₂ at 25 °C for 1 h gives **11**, converting a (CH₃)₂N-4'' into CH₃NH-4'' group, in 37% isolated yield. The crystal structure of **11** supports the molecular structure **10** possessing a partial structure *cis*-3,6-substituted 1,2-dimethoxycarbonyl-1,4-cyclohexadiene. The title basic studies on the above are reported in detail.

© 2010 Elsevier Ltd. All rights reserved.

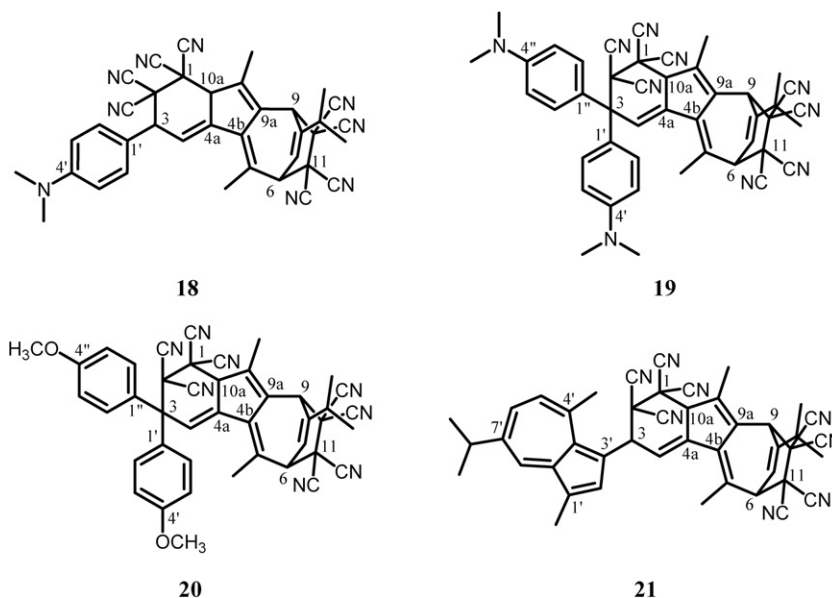
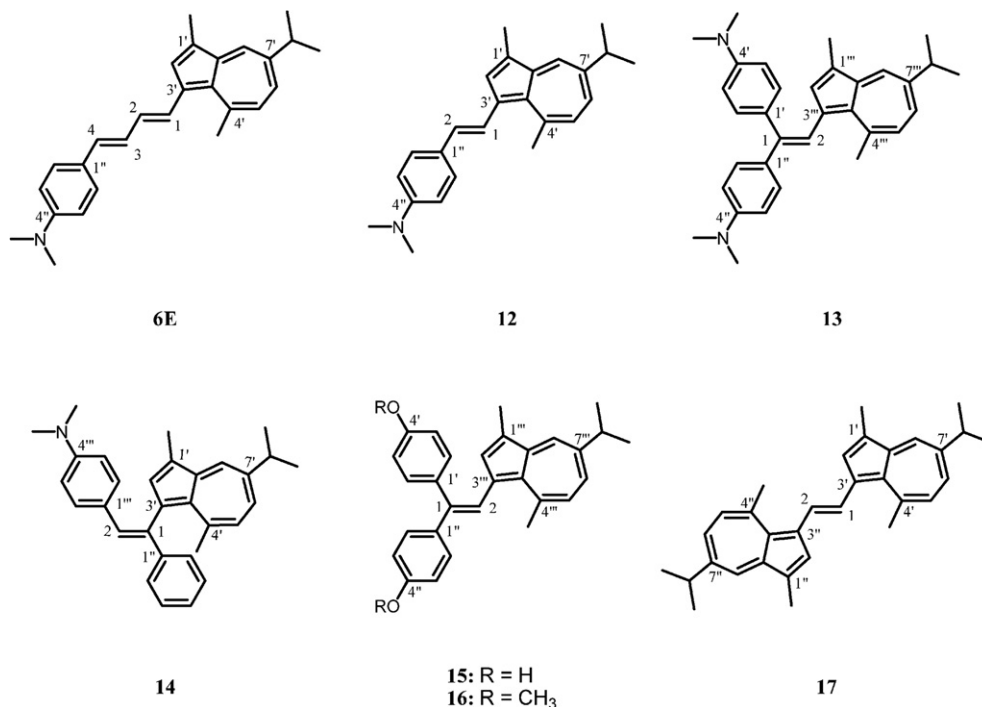
1. Introduction

In the previous papers,^{1–22} we reported facile preparation and crystal structures as well as spectroscopic, chemical, and electrochemical properties of new conjugated π -electron systems possessing a 3-guaiazulenyl (=5-isopropyl-3,8-dimethylazulen-1-yl)^{1–16,18–22} [or an azulene-1-yl^{8,15} or a 3-(methoxycarbonyl)azulen-1-yl¹⁷] group. During the course of our basic and systematic investigations on azulenes, we found that **12**,¹⁸ **13**,¹⁸ and **14–17**⁸ (see Chart 1) serve as strong two-electron donors and one-electron acceptors (or a two-electron acceptor for **17**), respectively, and further, that the reactions of **12**, **13**, **16**, and **17** with 2 equiv of TCNE, which serves as a strong electron acceptor,^{11,12} in benzene at 25 °C for 24 h under argon give unique cycloaddition products **18**,¹⁸ **19**,¹⁸ **20**,¹² and **21**¹² (see Chart 2),

possessing interesting molecular structures, selectively. Similar to our products **18–21**, in 2009 Shoji et al. reported that the reaction of 1,3,6-tri-*tert*-butylazulene with TCNE in ethyl acetate at room temperature for 15 h gave 3,5,9-tri-*tert*-butyltricyclo[6.2.2.0^{2,6}]-dodeca-2,4,6,9-tetraene-11,11,12,12-tetracarbonitrile,²³ quantitatively, whose proposed reaction mechanism was quoted from our literature.¹² Furthermore, in relation to the conjugated π -electron systems **12–17**, for example, preparation and anticancer activity of (*E*)-1-aryl-2-(3-guaiazulenyl)ethylenes and (2*E*,4*E*)-1-aryl-4-(3-guaiazulenyl)-1,3-butadienes have been reported²⁴ and moreover, preparation and anticoccidial activity,²⁵ quadratic nonlinear optical properties,^{26,27} fluorescence properties,^{28–30} and functional dyes³¹ of (*E*)-1-aryl-2-[4-(dimethylamino)phenyl]ethylenes and (2*E*,4*E*)-1-aryl-4-[4-(dimethylamino)phenyl]-1,3-butadienes have been studied to a considerable extent; however, none have really been documented for the accurate crystal structures as well as the detailed spectroscopic, chemical, and electrochemical properties of

* Corresponding author. Tel.: +81 6 6721 2332x5222; fax: +81 6 6727 2024.

E-mail address: takekuma@apch.kindai.ac.jp (S.-i. Takekuma).



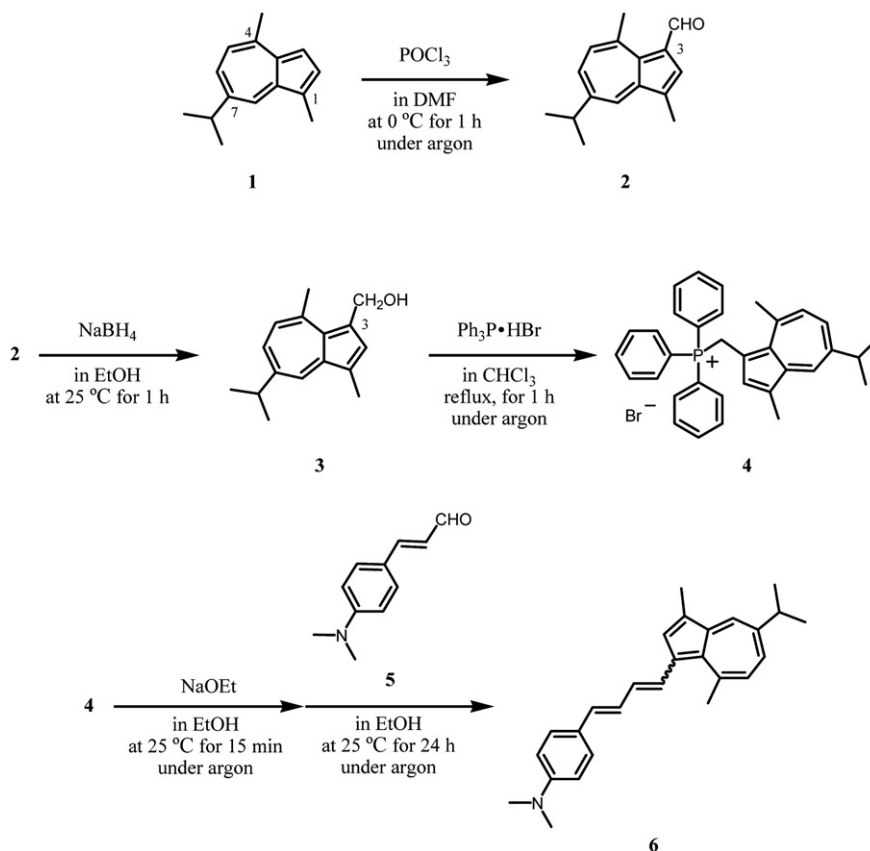
those compounds. Along with the above basic studies,^{1–31} our next challenge has quite recently been focused on the following clarification: namely, (i) preparation, crystal structure, and characteristic properties of the title new extended π -electron system **6E** (see **Chart 1**) compared with those of **12**. Especially, compound **6E**, formed by the C, H, N elements, can be expected to serve as a more strong two-electron donor in comparison with **12** and a similar one-electron acceptor to **12**, whose phenomena are noteworthy as an organic electronic material; (ii) a plausible redox mechanism based on the redox potentials of **6E**, compared with those of **12**, by means of cyclic voltammogram (CV) and differential pulse voltammogram (DPV); and (iii) the reaction of **6E** with TCNE under the same reaction conditions as for **12** and a plausible reaction pathway for the

formation of the resulting product. We now wish to report the detailed studies on clarification of the above (i)–(iii) with a view to comparative study and further, on the reactions of **6E** with DCNE (and DMAD) compared with the reaction of **6E** with TCNE.

2. Results and discussion

2.1. Preparation and spectroscopic properties of **6E** compared with those of **12**

In 2008 we reported preparation, crystal structure, and spectroscopic, chemical, and electrochemical properties of the 4-(dimethylamino)phenyl- and 3-guaiazulenylyl-substituted (*E*)-ethylene



Scheme 1. The preparation of the Wittig reagent **4** and the reaction of **5** with **4** in ethanol in the presence of sodium ethoxide at 25 °C for 24 h under argon.

derivative **12**¹⁸ (12% isolated yield) (see Chart 1) in detail. For comparative purposes, the 4-(dimethylamino)phenyl- and 3-guaiazulenyl-substituted (2*E*,4*E*)-1,3-butadiene derivative **6E** was prepared, in 19% isolated yield, using the Wittig reaction shown in Scheme 1. The molecular structure of **6E** was established on the basis of spectroscopic data [UV–vis, IR, exact EIMS, and ¹H and ¹³C NMR including 2D NMR (i.e., H–H COSY, HMQC, and HMBC)]. Similar to **12**, the geometrical isomer of **6E**, i.e., (2*Z*,4*E*)-4-[4-(dimethylamino)phenyl]-1-(3-guaiazulenyl)-1,3-butadiene (**6Z**), was observed by the silica gel TLC analysis of the reaction mixture,³² while it could not be isolated using silica gel column chromatography and recrystallization. The molecular structure of **6Z** could be determined by the ¹H NMR spectral analysis of a mixture of **6E** and **6Z**.³²

The target compound **6E** was obtained as black plates, while a solution of **6E** in CH₂Cl₂ was green. The spectroscopic properties of **6E** compared with those of **12** are described as follows. The UV–vis spectrum of **6E** showed that the spectral pattern of **6E**

resembled that of **12**; however, the longest absorption wavelength of **6E** revealed a slight bathochromic shift ($\Delta 5$ nm) and a slight hypochromic effect ($\Delta \log \epsilon = 0.03$) in comparison with that of **12** (see Fig. 1). These visible data corresponded to the $\Delta \pi$ -HOMO– π -LUMO/eV energy levels^{33,34} of **6E** and **12** (see Table 1). The IR spectrum showed specific bands based on the C–H, –HC=CH–, C=C, and C–N bonds, the wavenumbers of which revealed slight high and low wavenumber shifts in comparison with those of **12**. The molecular formula C₂₇H₃₁N was determined by exact EIMS spectrum. The ¹H NMR spectrum showed signals based on a 3-guaiazulenyl and 4-(dimethylamino)phenyl group and signals based on a (2*E*,4*E*)-1,3-butadiene unit possessing two substituents at the C-1 and C-4 positions, the signals of which were carefully assigned using H–H COSY and computer-assisted simulation based on first-order analysis. Although the proton signals (H-2'',6'' and H-1) of **6E** showed apparently up-field shifts in comparison with those of **12**, the other signals of **6E** coincided with those of **12**. The

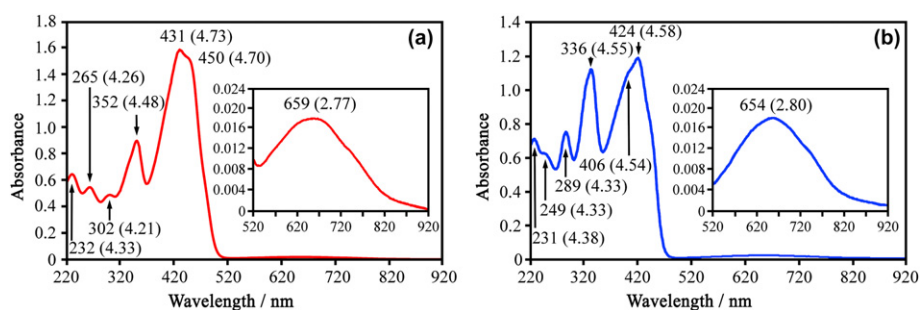


Figure 1. The UV–vis spectra of **6E** (a) and **12** (b) in CH₂Cl₂. Concentrations, **6E**: 0.11 g L⁻¹ (298 μmol), **12**: 0.10 g L⁻¹ (291 μmol). Length of the Cell, 0.1 cm each. Each log ϵ value is given in parenthesis.

Table 1

The dipole moments,^{33,34} the π -HOMO and π -LUMO energy levels,^{33,34} the longest wavelength absorption maxima, and the redox potentials^a of **6E** and **12**

Compound	Dipole moment/D	π -HOMO/eV	π -LUMO/eV	$\Delta \pi$ -HOMO- π -LUMO/eV
6E	1.963	-7.361	-1.056	-6.305
12	1.718	-7.464	-1.033	-6.431

Compound	λ_{\max} /nm (log ϵ)	E_{ox}^1 /V	E_{ox}^2 /V	E_{red}^1 /V
6E	659 (2.77)	0.30	0.30	-1.70
12	654 (2.80)	0.33	0.46	-1.68

^a CV data.

¹³C NMR spectrum exhibited 23 carbon signals assigned using HMQC and HMBC. Although the carbon (C-3' and C-1'') and carbon (C-1 and C-2) signals of **6E** showed apparently up- and down-field shifts in comparison with those of **12**, the other signals of **6E** coincided with those of **12**. Thus, the spectroscopic data for **6E** led to the molecular structure illustrated in Chart 1.

2.2. X-ray crystal structure of **6E** compared with that of **12**

The recrystallization of **6E** from a mixed solvent of chloroform and methanol (1:5, vol/vol) provided stable single crystals suitable for X-ray crystallographic analysis. The crystal structure of **6E** was then determined by means of X-ray diffraction, producing accurate structural parameters. As a result, two molecules of **6E** were found to exist in the unit cell of the crystal. The different views of the two ORTEP drawings (**6E^A** and **6E^B**) with a numbering scheme are shown in Figures 2a and b. Similar to **12**, the crystal structures of **6E^A** and **6E^B** supported the molecular structure (see Chart 1) established on the basis of spectroscopic data. Previously, it was found that the aromatic rings of the 4''-(dimethylamino)phenyl and 3'-guaiazulenyl groups of **12** twisted by 1° and 23° from the plane of the *trans*-HC=CH-unit, presumably due to the influence of inter-molecular stacking.¹⁸ Similar to **12**, each plane of the 3'-guaiazulenyl group, the C1-C2 part, and the C3-C4 part twisted by 17°, 1°, and 8° (for **6E^A**) and 12°, 8°, and 13° (for **6E^B**), respectively, from each plane of the C1-C2 part, the C3-C4 part, and the 4''-(dimethylamino)phenyl group, owing to a similar reason to that of **12**. The structural parameters of **6E^A** and **6E^B** showed that the average C-C bond lengths for the seven- and five-membered rings of the 3-guaiazulenyl groups of **6E^A** (1.410 and 1.429 Å) and **6E^B** (1.409 and 1.429 Å) coincided with those of **12** (1.407 and 1.425 Å). The C1-C2 and C3-C4 bond lengths of **6E^A** and **6E^B** were longer than the C1-C2 bond length of **12**. The bond alternation pattern observed for the 3-guaiazulenyl and 4-(dimethylamino)phenyl groups of **6E^A** and **6E^B** coincided with that of **12**, suggesting a small contribution of the resonance structures of the

3-guaiazulenyl and *p*-benzoquinodimethane monoiminium ions.¹⁸ Along with the experimental results, the accurate parameters for the crystal structures of **6E^B** and **12** were transferred to a WinMOPAC (Ver. 3.0) program³⁴ and their dipole moments and π -HOMO- π -LUMO energy levels were calculated,³³ each value of which was shown in Table 1. From the calculation, it is suggested that the dipole moment of **6E^B** (1.963 debye) is larger than that of **12** (1.718 debye), and that the $\Delta \pi$ -HOMO- π -LUMO energy level of **6E^B** (-6.305 eV) is smaller than that of **12** (-6.431 eV), the values of which coincide with the difference between the longest visible absorption wavelength of **6E** and that of **12**.

2.3. Electrochemical behavior of **6E** compared with that of **12**

The electrochemical property of **6E** was measured by means of CV and DPV [Potential (in volt) vs. SCE] in CH₃CN containing 0.1 M [*n*-Bu₄N]BF₄ as a supporting electrolyte. Two redox potentials observed by DPV were positioned at the E_p values of +0.31 and -1.68 V, whose currents showed 57.6 and 31.3 μ A, and the corresponding two reversible redox potentials determined by CV were located at the values of +0.30 ($E_{1/2}$) and -1.70 V ($E_{1/2}$) as shown in Figures 3a and b. The result of the DPV datum [i.e., the ratio of each current (in μ A) of the two redox potentials] showed that **6E** served as a two-electron donor and a one-electron acceptor. Furthermore, it was found that the reduction potential of **6E** coincided with that of **12**, and that **6E** underwent two-electron oxidation simultaneously, while **12** underwent stepwise two-electron oxidation.¹⁸ The reduction potentials of **6E** and **12** corresponded to their π -LUMO/eV energy levels and the oxidation potentials of **6E** and **12** corresponded to their π -HOMO/eV energy levels (see Table 1). Referring the π -HOMO and π -LUMO distribution diagrams on the ball and stick molecular structure of **6E^B** (see Fig. 4a and b)^{33,34} compared with those of **12** (Figs. 4c and d),^{33,34} a plausible redox mechanism of **6E** based on CV and DPV data can be inferred as illustrated in Scheme 2: namely, **6E** undergoes two-electron oxidation at a potential of +0.30 V ($E_{1/2}$) by CV (+0.31 V by DPV), generating an electrochemically stable dication **6c** via the cation-radical **6a** and **6b**. Along with the oxidation potential, **6E** is reduced to the anion-radical **6d** at a potential of -1.70 V ($E_{1/2}$) by CV (-1.68 V by DPV). In conclusion, we clarified that **6E** serves as a more strong two-electron donor in comparison with **12** and a similar one-electron acceptor to **12**.

2.4. Reaction of **6E** with TCNE

In 2008 we reported that the reaction of **12** with 2 equiv of TCNE in benzene at 25 °C for 24 h under argon gave a product **18** (see Chart 2) in 41% isolated yield and further, a plausible reaction

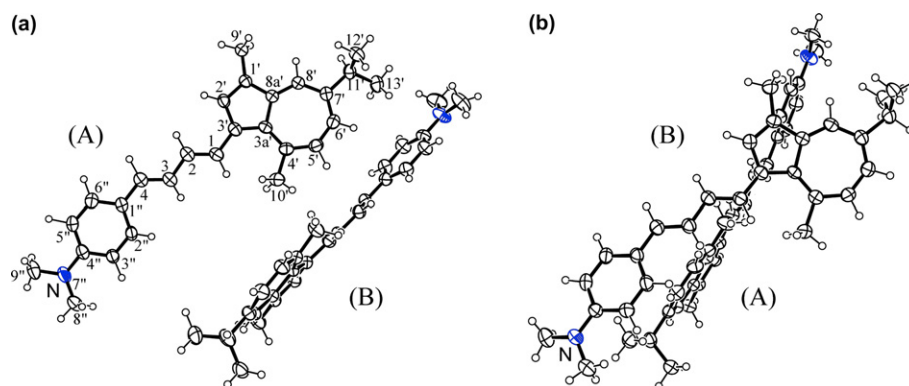


Figure 2. The different views of the ORTEP drawings, with a numbering scheme (30% probability thermal ellipsoids), of **6E^A** and **6E^B**.

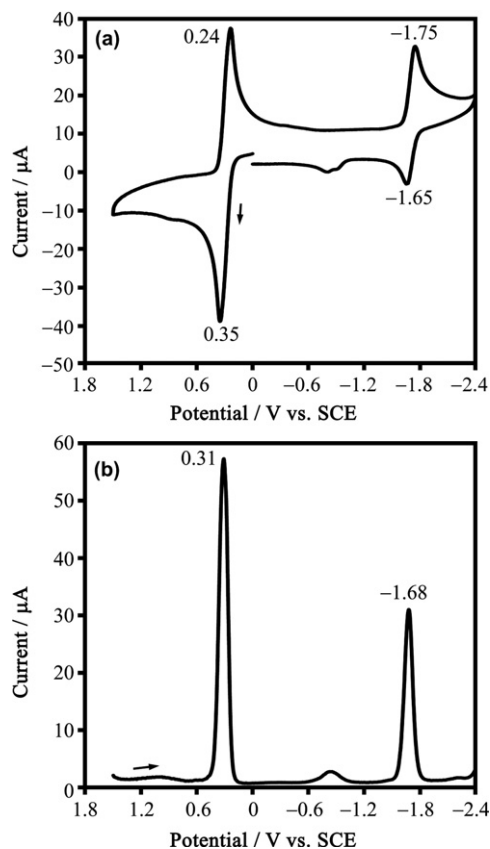


Figure 3. Cyclic and differential pulse voltammograms of **6E** (2.9 mg, 7.8 μmol) [see (a), (b)] in 0.1 M $[n\text{-Bu}_4\text{N}]\text{BF}_4$, CH_3CN (10 mL) at a glassy carbon (ID: 3 mm) and a platinum wire served as the working and auxiliary electrodes; scan rates 100 mV s^{-1} at 25 $^\circ\text{C}$ under argon. For comparative purposes, the oxidation potential using ferrocene as a standard material showed +0.45 V (E_p) by DPV and +0.42 V ($E_{1/2}$) by CV under the same electrochemical measurement conditions as for **6E**.

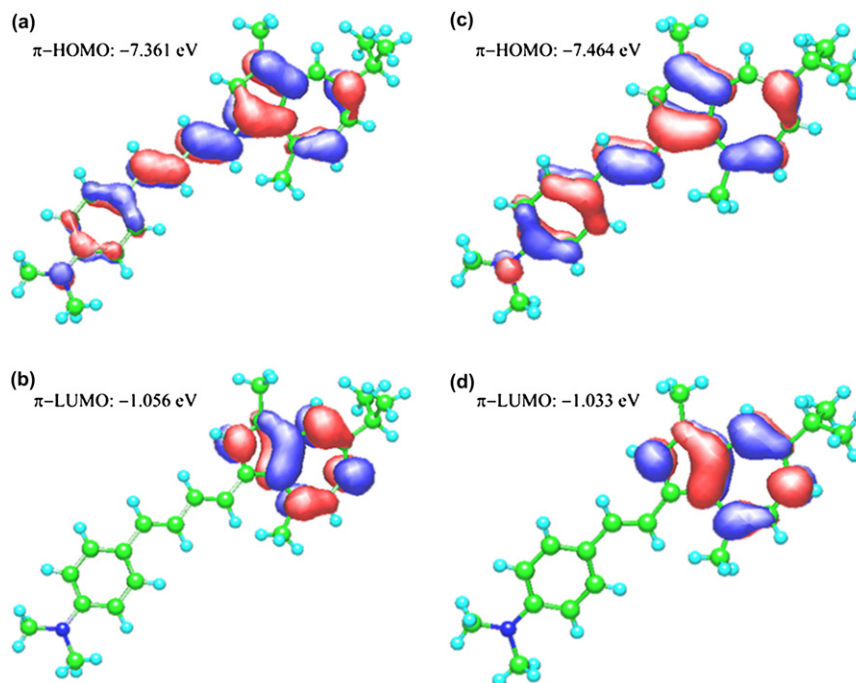
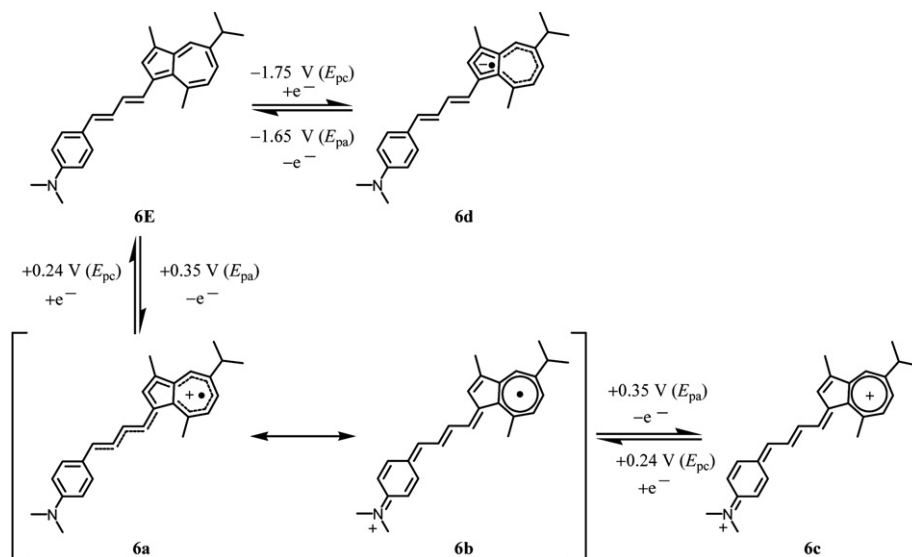


Figure 4. The π -HOMO and π -LUMO energy levels of **6E** [see (a), (b)] and **12** [see (c), (d)], and their distribution diagrams on the ball and stick molecular structures of **6E** [see (a), (b)] and **12** [see (c), (d)].

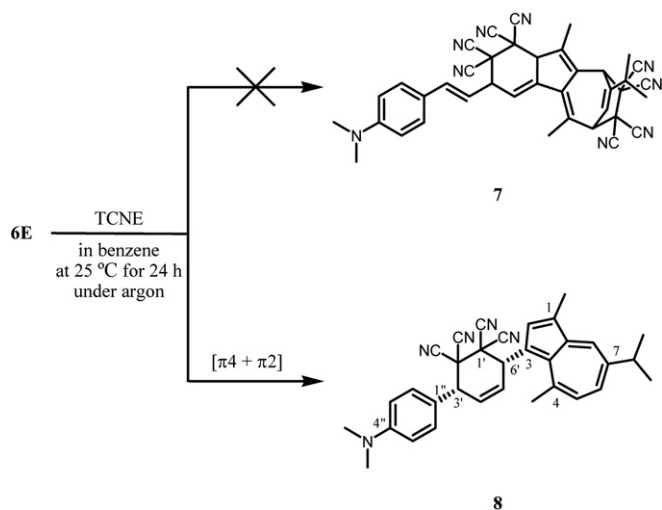
pathway for the formation of **18** was proposed. Along with the spectroscopic properties of **18**, the crystal structure of **18** was determined.¹⁸ For comparative purposes, the reaction of **6E** with 2 equiv of TCNE was carried out under the same reaction conditions as for **12**¹⁸ (see Scheme 3), affording a new $[\pi 4+\pi 2]$ cycloaddition product **8**³⁵ in 59% isolated yield, the molecular structure of which was established on the basis of similar spectroscopic analyses to those of **6E**. This reaction did not give a structurally unique product **7** (see Scheme 3), which is a similar adduct to **18–21** (see Chart 2).

Compound **8** was obtained as blue plates. The characteristic UV–vis absorption bands of **6E** were not observed, while those based on guaiazulene³⁶ (=7-isopropyl-1,4-dimethylazulene) (**1**) with two bands (434 and 453 nm) were observed as shown in Figure 5 and the longest visible absorption wavelength appeared at λ_{max} 592 nm ($\log \epsilon=2.68$). The IR spectrum showed specific bands from the C–H, $\text{C}\equiv\text{N}$, C=C, and C–N bonds. The molecular formula $\text{C}_{33}\text{H}_{31}\text{N}_5$ was determined by exact FABMS spectrum. The ^1H NMR (including NOE) spectrum showed signals based on a 4-(dimethylamino)-phenyl and 3-guaiazulenyl group and a *cis*-3,6-substituted 1,1,2,2-tetracyano-4-cyclohexene unit, the signals of which were carefully assigned using conventional methodology. The ^{13}C NMR spectrum exhibited 38 carbon signals assigned using HMQC and HMBC. Thus, the spectroscopic data for **8** led to the molecular structure illustrated in Scheme 3. In relation to our study, in 1990 O’Shea and Foote reported that the reaction of (2*E*,4*E*)-hexadiene with TCNE in CH_2Cl_2 at 25 $^\circ\text{C}$ yielded the Diels–Alder adduct 1,1,2,2-tetracyano-*cis*-3,6-dimethyl-4-cyclohexene, quantitatively (>99.5% yield),³⁷ the partial structure *cis*-3,6-substituted 1,1,2,2-tetracyano-4-cyclohexene, established on the basis of ^1H NMR spectral analysis, of which coincided with that of **8**.

The recrystallization of **8** from a mixed solvent of ethyl acetate and hexane (1:5, vol/vol) provided stable single crystals suitable for X-ray crystallographic analysis. The crystal structure of **8** was then determined by means of X-ray diffraction, producing accurate structural parameters. As a result, a molecule of the *cis*-3,6-substituted form **8** with an equivalent of AcOEt molecule was found to exist in the unit cell of the crystal. The ORTEP drawing with



Scheme 2. A plausible redox mechanism based on the CV and DPV data of **6E** and the π -HOMO- π -LUMO distribution diagrams on the ball and stick molecular structure of **6E**.



Scheme 3. The reaction of **6E** with 2 equiv of TCNE in benzene at 25 °C for 24 h under argon.

a numbering scheme, indicating the molecular structure **8** illustrated in Scheme 3, is shown in Figure 6.

2.5. A plausible reaction pathway for the formation of **8**

In 2008 we proposed a plausible reaction pathway for the formation of **18** and **19** illustrated in Scheme 4:¹⁸ namely, to a solution

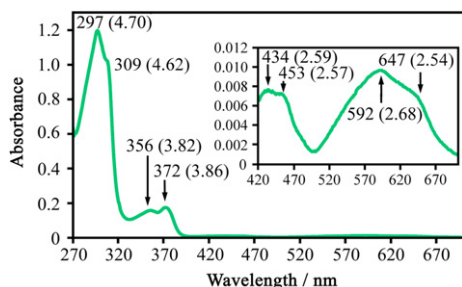


Figure 5. The UV-vis spectrum of **8** in benzene. Concentration, **8** with an equivalent of AcOEt molecule: 0.14 g L⁻¹ (239 μmol). Length of the Cell, 0.1 cm. Each log ϵ value is given in parenthesis.

of TCNE in benzene was added a solution of **12** (or **13**) in benzene under argon, turning the green solution of **12** (or **13**) into a black solution, rapidly. The result suggested that the reaction of **12** (or **13**) with TCNE gave the corresponding charge-transfer (CT) complex **a**. Following addition, the reaction mixture was stirred at 25 °C for 24 h under argon, gradually precipitating a white solid of **18** (or **19**). As it so happens, azulenes are unsusceptible to Diels-Alder reaction.³⁸ Thus, these results suggested that the CT complex **a** was converted to **18** (or **19**), presumably via the biradical **b**, the intermediate **c**, and the $[\pi 4+\pi 2]$ cycloaddition of **c** with TCNE.¹⁸

For a comparative purpose, we now propose a plausible reaction pathway for the formation of **8** according to the following experimental results: namely, to a solution of TCNE in benzene was added a solution of **6E** in benzene under argon, turning the green solution of **6E** into a blue solution of **8**, rapidly. From the visible spectra of this reaction shown in Figure 7, a plausible reaction pathway for formation can be inferred that compound **8** is produced presumably via the Diels-Alder (i.e., the $[\pi 4+\pi 2]$ cycloaddition) reaction of **6E** with TCNE (see Scheme 3).

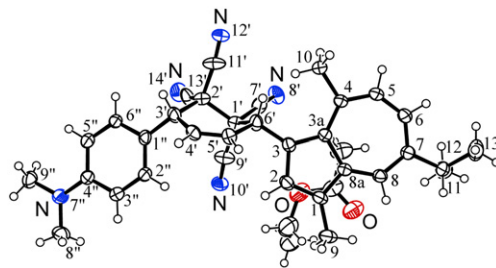
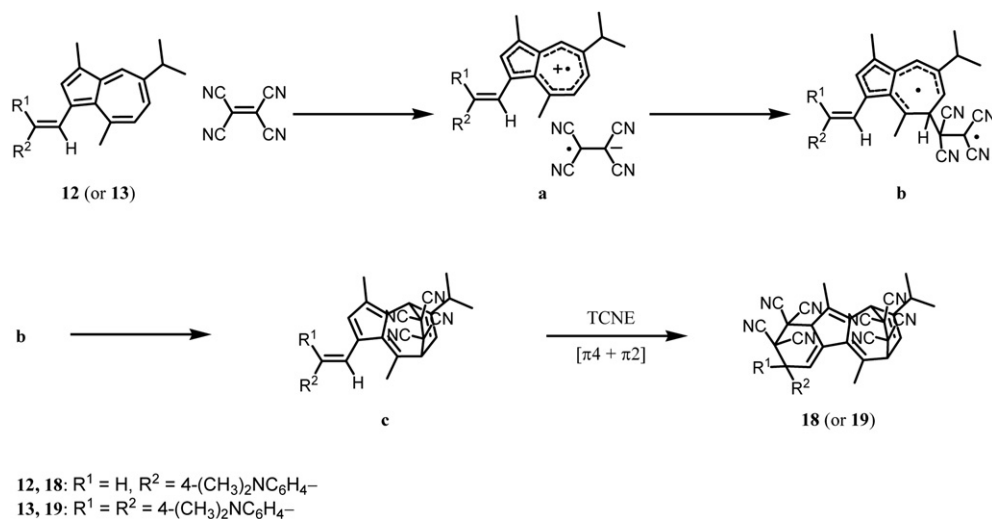


Figure 6. The ORTEP drawing, with a numbering scheme (30% probability thermal ellipsoids), of **8** possessing an equivalent of AcOEt molecule. The selected bond lengths (Å) of **8** are as follows: C1–C2; 1.389(3), C2–C3; 1.428(3), C3–C3a; 1.416(2), C3a–C4; 1.411(2), C4–C5; 1.517(3), C4–C5; 1.402(3), C5–C6; 1.391(3), C6–C7; 1.396(3), C7–C11; 1.528(3), C11–C12; 1.521(4), C11–C13; 1.529(4), C7–C8; 1.403(3), C8–C8a; 1.386(3), C8a–C1; 1.419(3), C1–C9; 1.499(3), C3a–C8a; 1.500(2), C1'–C7'; 1.498(3), C7'–N8'; 1.132(3), C1'–C9'; 1.477(3), C9'–N10'; 1.122(2), C1'–C2'; 1.594(3), C2'–C11'; 1.479(3), C11'–N12'; 1.136(4), C2'–C13'; 1.497(4), C13'–N14'; 1.135(4), C2'–C3'; 1.576(3), C3'–C4'; 1.505(3), C4'–C5'; 1.332(3), C5'–C6'; 1.508(2), C6'–C1'; 1.620(3), C6'–C3; 1.491(3), C3'–C1''; 1.517(3), C1''–C2''; 1.393(3), C2''–C3''; 1.389(3), C3''–C4''; 1.414(3), C4''–N7''; 1.369(3), N7''–C8''; 1.443(3), N7''–C9''; 1.445(3), C4''–C5''; 1.412(3), C5''–C6''; 1.386(3), and C6''–C1''; 1.402(3).



Scheme 4. A plausible reaction pathway for the formation of **18** (or **19**).

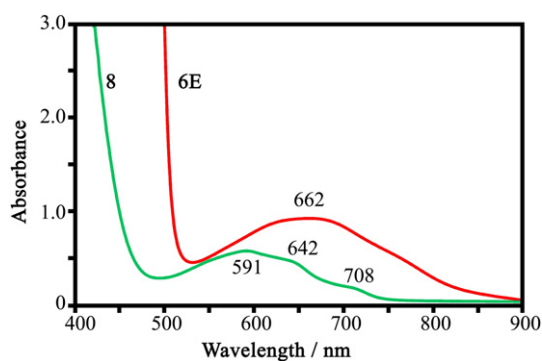
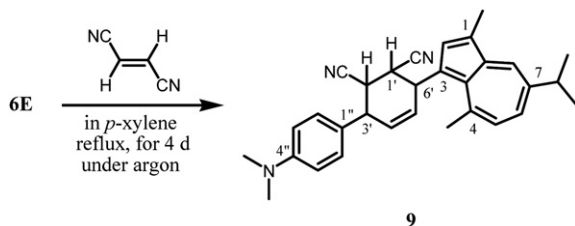


Figure 7. The visible spectra of the reaction of **6E** (red solid line) with TCNE in benzene under argon, giving a product **8** (green solid line), selectively. Length of the Cell, 1.0 cm. Reaction conditions: to a solution of TCNE (0.7 mg, 5.5 μmol) in benzene (1 mL) was added a solution of **6E** (1.0 mg, 2.7 μmol) in benzene (2 mL) at 25 °C under argon, turning the green solution of **6E** into a blue solution of **8**, rapidly.

2.6. Reaction of **6E** with DCNE

For comparative purposes, the reaction of **6E** with DCNE was carried out under the same reaction conditions as for the reaction of **6E** with TCNE, the reaction of which gave no product. This reaction in toluene at reflux temperature (110 °C) for four days under argon afforded a new Diels–Alder adduct **9** very slightly, while the reaction in *p*-xylene at reflux temperature (138 °C) for four days under argon yielded **9** in 54% isolated yield (see Scheme 5), owing to the influence of reaction temperature. The molecular structure of **9** was established on the basis of similar spectroscopic analyses to those of **8**.



Scheme 5. The reaction of **6E** with DCNE in *p*-xylene at reflux temperature (138 °C) for four days under argon.

Compound **9** was obtained as blue needles. Similar to **8**, the characteristic UV–vis absorption bands of **6E** were not observed,

while those based on guaiazulene³⁶ were observed as shown in Figure 8 and the longest visible absorption wavelength appeared at λ_{max} 609 nm (log ε=2.78). The IR spectrum showed specific bands from the C–H, C≡N, C=C, and C–N bonds. The molecular formula C₃₁H₃₃N₃ was determined by exact FABMS spectrum. The ¹H NMR spectrum showed signals based on a 4-(dimethylamino)phenyl and 3-guaiazulenyl group and a 1,2-dicyano-4-cyclohexene unit possessing two substituents at the C-3 and C-6 positions, the signals of which were carefully assigned using conventional methodology. Careful study of the ¹H NMR signals suggested a ca. 5:3, mixture of chromatographically inseparable diastereomers **9a** and **9b** (see Experimental section 4.1.6). The ¹³C NMR spectrum exhibited 25 (for **9a**) and 26 (for **9b**) carbon signals assigned using HMQC and HMBC. Thus, the spectroscopic data for **9** led to the molecular structure illustrated in Scheme 5. A similar reaction pathway to that of **8** can be inferred for the formation of **9**.

2.7. Reaction of **6E** with DMAD

For comparative purposes, the reaction of **6E** with DMAD was carried out under the same reaction conditions as for the reaction of **6E** with TCNE, the reaction of which gave no product; however, this reaction in toluene at reflux temperature (110 °C) for two days under argon afforded a new Diels–Alder adduct **10** in 58% isolated yield (see Scheme 6), owing to the influence of reaction temperature. The molecular structure of **10** was established on the basis of similar spectroscopic analyses to those of **8**. In relation to our study, in 1994 Coudert et al. reported that the reactions of (2*E*,4*E*)-1,3-

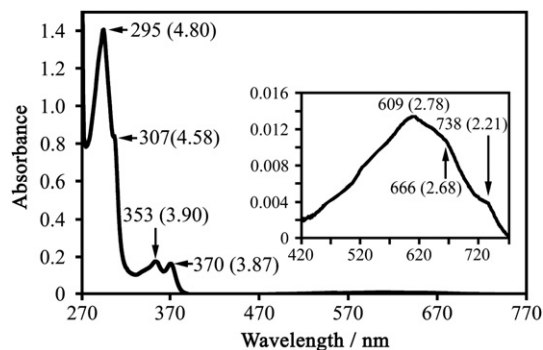
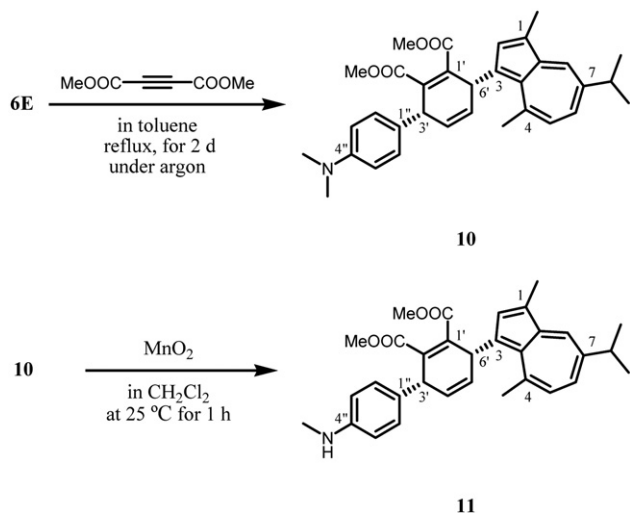


Figure 8. The UV–vis spectrum of **9** in benzene. Concentration, **9**: 0.10 g L⁻¹ (223 μmol). Length of the Cell, 0.1 cm. Each log ε value is given in parenthesis.

butadiene derivatives with dimethyl acetylenedicarboxylate at 130–150 °C for 15 min–1 h yielded similar Diels–Alder adducts to **10** in 51–82% isolated yields,³⁹ each partial structure *cis*-3,6-substituted 1,2-dimethoxycarbonyl-1,4-cyclohexadiene, established on the basis of ¹H NMR spectral analysis, of which coincided with that of **10**.



Scheme 6. The reaction of **6E** with DMAD in toluene at reflux temperature (110 °C) for two days gives **10**, which upon oxidation with MnO₂ in CH₂Cl₂ at 25 °C for 1 h affords **11**.

Compound **10** was obtained as a blue solid. Similar to **8**, the characteristic UV–vis absorption bands of **6E** were not observed, while those based on guaiazulene³⁶ were observed as shown in Figure 9 and the longest visible absorption wavelength appeared at λ_{\max} 616 nm (log ϵ = 2.73). The molecular formula C₃₃H₃₇O₄N was determined by exact FABMS spectrum. The ¹H NMR (including NOE) spectrum showed signals based on a 4-(dimethylamino)-phenyl and 3-guaiazulenyl group and a *cis*-3,6-substituted 1,2-dimethoxycarbonyl-1,4-cyclohexadiene unit, the signals of which were carefully assigned using conventional methodology. The ¹³C NMR spectrum exhibited 29 carbon signals assigned using HMQC and HMBC. Thus, the spectroscopic data for **10** led to the molecular structure illustrated in Scheme 6. A similar reaction pathway to that of **8** can be inferred for the formation of **10**.

We have further found that the oxidation of **10** with MnO₂ in CH₂Cl₂ at 25 °C for 1 h gives **11**, converting a (CH₃)₂N-4'' into CH₃NH-4'' group, in 37% isolated yield (see Scheme 6). Although it was very difficult to obtain a single crystal of **10** suitable for X-ray crystallographic analysis, recrystallization of **11** from a mixed solvent of hexane and ethyl acetate (5:1, vol/vol) provided a single crystal suitable for that purpose. The crystal structure of **11** was

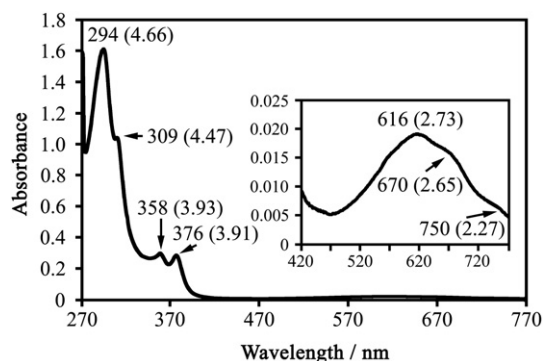


Figure 9. The UV–vis spectrum of **10** in benzene. Concentration, **10**: 0.18 g L⁻¹ (352 μ mol). Length of the Cell, 0.1 cm. Each log ϵ value is given in parenthesis.

$d = 2.57 \text{ \AA}$

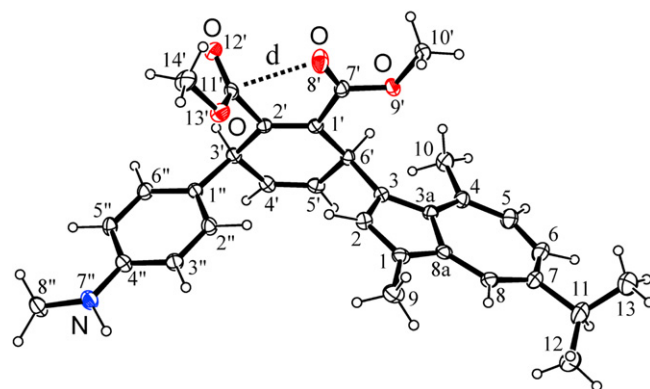


Figure 10. The ORTEP drawing, with a numbering scheme (30% probability thermal ellipsoids), of **11**. The selected bond lengths (Å) of **11** are as follows: C1–C2; 1.384(4), C2–C3; 1.400(4), C3–C3a; 1.409(4), C3a–C4; 1.413(4), C4–C5; 1.403(5), C5–C6; 1.379(5), C6–C7; 1.374(6), C7–C8; 1.394(6), C8–C8a; 1.391(4), C8a–C1; 1.411(5), C3a–C8a; 1.498(4), C1–C9; 1.501(4), C4–C10; 1.515(4), C7–C11; 1.510(6), C11–C12; 1.418(7), C11–C13; 1.475(7), C1'–C2'; 1.347(4), C2'–C3'; 1.522(3), C3'–C4'; 1.505(4), C4'–C5'; 1.324(4), C5'–C6'; 1.520(4), C6'–C1'; 1.501(4), C1'–C7'; 1.501(4), C7'–O8'; 1.203(4), C7'–O9'; 1.332(3), O9'–C10'; 1.440(3), C2'–C11'; 1.499(4), C11'–O12'; 1.208(3), C11'–O13'; 1.336(3), O13'–C14'; 1.445(4), C6'–C3; 1.533(3), C3'–C1''; 1.520(4), C1''–C2''; 1.391(4), C2''–C3''; 1.375(4), C3''–C4''; 1.390(4), C4''–C5''; 1.397(4), C5''–C6''; 1.392(4), C6''–C1''; 1.389(4), C4''–N7''; 1.375(4), and N7''–C8''; 1.425(4).

then determined by means of X-ray diffraction, producing accurate structural parameters. The ORTEP drawing with a numbering scheme is shown in Figure 10, indicating the molecular structure **11** illustrated in Scheme 6. It is found that the methoxycarbonyl group at the C1' position is upright against the other methoxycarbonyl group at the C2' position and the distance between the C11' and O8' atoms is 2.57 Å, suggesting the formation of the C^{δ+}...O^{δ-} coordinate bond. Thus, the crystal structure of **11** supported the molecular structure **10**, possessing a partial structure *cis*-3,6-substituted 1,2-dimethoxycarbonyl-1,4-cyclohexadiene, illustrated in Scheme 6.

3. Conclusion

We have reported the following ten interesting points for the title basic studies: namely, (i) the Wittig reaction of the aldehyde **5** with the reagent **4** in ethanol containing NaOEt at 25 °C for 24 h under argon gave the title new (*2E,4E*)-1,3-butadiene derivative **6E** in 19% isolated yield; (ii) the spectroscopic data of **6E** compared with those of the previously reported (*E*)-ethylene derivative **12** were documented and further, the longest visible absorption wavelengths of **6E** and **12** corresponded to their $\Delta\pi$ -HOMO– π -LUMO/eV energy levels; (iii) the crystal structure of **6E** could be determined, supporting the molecular structure established on the basis of spectroscopic data, the accurate structural parameters of which enabled us to compare with those of **12**; (iv) similar to **12**, the electrochemical behavior of **6E** showed that it serves as a more strong two-electron donor in comparison with **12** and a similar one-electron acceptor to **12** and further, the redox potentials of **6E** and **12** corresponded to their π -HOMO and π -LUMO/eV energy levels; (v) a redox mechanism based on the redox potentials and the π -HOMO and π -LUMO distribution diagrams of **6E** compared with those of **12** was proposed; (vi) although the reaction of **6E** with 2 equiv of TCNE in benzene at 25 °C for 24 h under argon did not give **7** possessing a similar structure to **18–21**, the reaction afforded a new Diels–Alder adduct **8**, in 59% isolated yield; (vii) along with the spectroscopic properties of **8**, the crystal structure of **8** could be determined, supporting the 3,6-*cis*-form established on the basis of spectroscopic data, and further, a reaction pathway for

the formation of **8** via Diels–Alder reaction was proposed; (viii) the reaction of **6E** with DCNE under the same reaction conditions as for the reaction of **6E** with TCNE gave no product; however, this reaction in *p*-xylene at reflux temperature (138 °C) for four days under argon afforded a new Diels–Alder adduct **9**, in 54% isolated yield, owing to the influence of reaction temperature; (ix) although the reaction of **6E** with DCNE in toluene at reflux temperature (110 °C) for four days under argon provided **9** very slightly, the reaction of **6E** with DMAD in toluene at reflux temperature for two days under argon yielded a new Diels–Alder adduct **10**, in 58% isolated yields, which upon oxidation with MnO₂ in CH₂Cl₂ at 25 °C for 1 h gave **11**, converting a (CH₃)₂N-4'' into CH₃NH-4'' group, in 37% isolated yield. The crystal structure of **11** supported the molecular structure **10** possessing a partial structure *cis*-3,6-substituted 1,2-dimethoxycarbonyl-1,4-cyclohexadiene; and (x) a similar reaction pathway to that of **8** could be inferred for the formation of **9** and **10**.

4. Experimental

4.1. General

Melting points were taken on a Yanagimoto MP-S3 instrument. FAB- and EIMS spectra were taken on a JEOL The Tandem Mstation JMS-700 TKM data system. UV–vis and IR spectra were taken on a Beckman DU640 spectrophotometer and a Shimadzu FTIR-4200 Grating spectrometer. NMR spectra were recorded with a JEOL GX-500 (500 MHz for ¹H and 125 MHz for ¹³C) and JNM-ECA700 (700 MHz for ¹H and 176 MHz for ¹³C) cryospectrometer at 25 °C. ¹H NMR spectra were assigned using computer-assisted simulation (software: gNMR developed by Adept Scientific plc) on a DELL Dimension 9150 personal computer with a Pentium IV processor. Cyclic and differential pulse voltammograms (CV and DPV) were measured with an ALS Model 600 electrochemical analyzer.

4.1.1. Preparation of (3-guaiazulenylmethyl)triphenylphosphonium bromide (4). Guaiazulene-3-carbaldehyde (=5-isopropyl-3,8-dimethylazulene-1-carbaldehyde) (**2**), which is a synthetic intermediate of the Wittig reagent **4**, was prepared according to the following procedure: namely, to a solution of commercially available guaiazulene (=7-isopropyl-1,4-dimethylazulene) (**1**) (100 mg, 504 μmol) in *N,N*-dimethylformamide (DMF) (3 mL) was added a solution of phosphoryl chloride (100 μL). The mixture was stirred at 0 °C for 1 h. After the reaction, the reaction solution was carefully neutralized with aq KOH and then the resulting product was extracted with dichloromethane (10 mL×3). The extract was washed with distilled water, dried (Na₂SO₄), and evaporated in vacuo. The residue thus obtained was carefully separated by silica gel column chromatography with hexane/ethyl acetate (3:2, vol/vol). The crude product was recrystallized from hexane to provide pure **2** as stable crystals (108 mg, 477 μmol, 94% yield). Continuously, the Wittig reagent **4** was prepared according to the following procedure: namely, to a powder of NaBH₄ (30 mg, 793 μmol) was added a solution of **2** (90 mg, 397 μmol) in ethanol (1.5 mL). The mixture was stirred at 25 °C for 1 h. After the reaction, distilled water (10 mL) was added to the mixture and then the resulting product was extracted with dichloromethane (10 mL×3). The extract was washed with distilled water, dried (Na₂SO₄), and evaporated in vacuo to provide pure 3-guaiazulenylmethanol (**3**) as a blue paste, quantitatively. To a solution of the obtained **3** in chloroform (3 mL) was added a solution of triphenylphosphonium bromide (130 mg, 378 μmol) in chloroform (3 mL). The mixture was refluxed for 1 h under argon. After cooling, the reaction mixture was poured into diethyl ether (10 mL), precipitating a blue solid, and then was centrifuged at 2.5 krpm for 1 min. The obtained product was

carefully washed with diethyl ether to provide pure **4** as a blue powder (195 mg, 352 μmol, 93% yield).

4.1.2. Preparation of (2E,4E)-4-[4-(dimethylamino)phenyl]-1-(3-guaiazulenyl)-1,3-butadiene (6E). To a solution of commercially available 3-[4-(dimethylamino)phenyl]propanal (**5**) (32 mg, 183 μmol) in ethanol (5 mL) was added a solution of (3-guaiazulenylmethyl)triphenylphosphonium bromide (**4**) (100 mg, 181 μmol) in ethanol (5 mL) containing sodium ethoxide (25 mg, 367 μmol). The mixture was stirred at 25 °C for 24 h under argon. After the reaction, distilled-water was added to the mixture, and then the resulting product was extracted with dichloromethane (20 mL×3). The extract was washed with distilled-water, dried (MgSO₄), and evaporated in vacuo. The residue thus obtained was carefully separated by silica gel column chromatography with hexane/ethyl acetate (9:1, vol/vol) as an eluant. The crude product **6** was recrystallized from methanol/chloroform (5:1, vol/vol) (several times) to provide pure **6E** (13 mg, 35 μmol, 19% yield) as stable single crystals.

Compound 6E: Black plates [*R*_f=0.19 on silica gel TLC (solv. hexane/ethyl acetate=9:1, vol/vol)]; mp 176 °C; UV–vis λ_{max}/nm (log ε) in CH₂Cl₂, 232 (4.33), 265 (4.26), 302 (4.21), 352 (4.48), 431 (4.73), 450sh (4.70), and 659 (2.77); IR ν_{max}/cm⁻¹ (KBr), 2955–2800 (C–H), 2955, 980 (–HC=CH–), 1601, 1520 (C=C), and 1354 (C–N); exact EIMS (70 eV), found: *m/z* 369.2477; calcd for C₂₇H₃₁N: M⁺, *m/z* 369.2457; 500 MHz ¹H NMR (benzene-*d*₆), signals based on a 3-guaiazulenyl group: δ 1.19 (6H, d, *J*=6.9 Hz, (CH₃)₂CH-7'), 2.523 (3H, br s, Me-1'), 2.71 (1H, sept, *J*=6.9 Hz, (CH₃)₂CH-7'), 2.81 (3H, s, Me-4'), 6.55 (1H, *J*=10.3 Hz, H-5'), 6.97 (1H, dd, *J*=10.3, 2.0 Hz, H-6'), 7.93 (1H, d, *J*=2.0 Hz, H-8'), and 7.98 (1H, br s, H-2'); signals based on a 4-(dimethylamino)phenyl group: δ 2.519 (6H, s, (CH₃)₂N-4''), 6.61 (2H, dd, *J*=8.9, 2.4 Hz, H-3'',5''), and 7.47 (2H, dd, *J*=8.9, 2.4 Hz, H-2'',6''); and signals based on a (2E,4E)-1,3-butadiene unit: δ 6.77 (1H, d, *J*=14.9 Hz, H-4), 7.07 (1H, dd, *J*=14.9, 10.5 Hz, H-2), 7.15 (1H, dd, *J*=14.9, 10.5 Hz, H-3), and 7.67 (1H, d, *J*=14.9 Hz, H-1); 125 MHz ¹³C NMR (benzene-*d*₆), δ 150.1 (C-4''), 146.4 (C-4'), 141.6 (C-8a'), 140.6 (C-7'), 136.4 (C-2'), 134.7 (C-6'), 133.4 (C-8'), 132.8 (C-3a'), 131.2 (C-4), 129.2 (C-2), 128.7 (C-1), 127.7 (C-2'',6''), 127.5 (C-3), 127.4 (C-1''), 127.3 (C-5'), 126.5 (C-1'), 126.5 (C-3'), 113.0 (C-3'',5''), 40.1 ((CH₃)₂N-4''), 37.9 ((CH₃)₂CH-7'), 28.4 (Me-4'), 24.4 ((CH₃)₂CH-7'), and 13.1 (Me-1').

4.1.3. X-ray crystal structure of (2E,4E)-4-[4-(dimethylamino)phenyl]-1-(3-guaiazulenyl)-1,3-butadiene (6E). A total 10,197 reflections with 2θ_{max}=55.0° were collected on a Rigaku AFC-5R automated four-circle diffractometer with graphite mono-chromated Mo Kα radiation (λ=0.71069 Å, rotating anode: 50 kV, 180 mA) at –75 °C. The structure was solved by direct methods (SIR92) and expanded using Fourier techniques (DIRDIF99). Non-hydrogen atoms were refined anisotropically. Hydrogen atoms were included but not refined. The final cycle of full-matrix least-squares refinement was based on *F*². All calculations were performed using the teXsan crystallographic software package. Crystallographic data have been deposited with Cambridge Crystallographic Data Center: Deposition number CCDC-669534 for compound No. **6E**. Copies of the data can be obtained free of charge via <http://www.ccdc.cam.ac.uk/conts/retrieving.html> (or from the Cambridge Crystallographic Data Centre, 12, Union Road, Cambridge, CB2 1EZ, UK; Fax: +44 1223 336033; e-mail: deposit@ccdc.cam.ac.uk).

Crystallographic data for **6E**: C₂₇H₃₁N (FW=369.55), black plate (crystal size, 1.00×0.60×0.30 mm³), triclinic, *P*-1 (#2), *a*=14.753(5) Å, *b*=17.080(5) Å, *c*=9.585(4) Å, α=99.86(3)°, β=108.74(3)°, γ=69.46(2)°, *V*=2137.1(13) Å³, *Z*=4, *D*_{calcd}=1.148 g/cm³, μ(Mo Kα)=0.653 cm⁻¹, scan width=(1.42+0.30 tanθ)°, scan mode=ω–2θ, scan rate=16.0°/min, measured reflections=10,197, observed

reflections=9817, No. of parameters=568, $R1=0.0523$, $wR2=0.1758$, goodness of fit indicator=0.983.

4.1.4. Reaction of (2E,4E)-4-[4-(dimethylamino)phenyl]-1-(3-guaiazulenyl)-1,3-butadiene (6E) with 1,1,2,2-tetracyanoethylene (TCNE). To a solution of compound **6E** (15 mg, 41 μmol) in benzene (2 mL) was added a solution of TCNE (10 mg, 78 μmol) in benzene (2 mL) under argon, turning the green solution of **6E** into a blue solution, rapidly. The mixture was stirred at 25 °C for 24 h under argon. After the reaction, the reaction solution was evaporated in vacuo. The crude product thus obtained was recrystallized from ethyl acetate/hexane (5:1, vol/vol) (several times) to provide pure 3-{1,1,2,2-tetracyano-*cis*-3-[4-(dimethylamino)phenyl]-4-cyclohexen-6-yl}guaiazulene (**8**), with an equivalent of AcOEt molecule, as stable single crystals (14 mg, 24 μmol , 59% yield).

Compound 8: Blue plates [$R_f=0.30$ on silica gel TLC (solvent: hexane/ethyl acetate=3:1, vol/vol)]; mp 223 °C; UV-vis $\lambda_{\text{max}}/\text{nm}$ (log ϵ) in benzene, 297 (4.70), 309sh (4.62), 356 (3.82), 372 (3.86), 434 (2.59), 453sh (2.57), 592 (2.68), and 647sh (2.54); IR $\nu_{\text{max}}/\text{cm}^{-1}$ (KBr), 2963–2812 (C–H), 2249 (C \equiv N), 1612, 1528 (C=C), and 1366 (C–N); exact FABMS (3-nitrobenzyl alcohol matrix), found: m/z 497.2589; calcd for $\text{C}_{33}\text{H}_{31}\text{N}_5$: M^+ , m/z 497.2579; 700 MHz ^1H NMR (benzene- d_6), signals based on a 3-guaiazulenyl group: δ 1.12 (6H, d, $J=6.9$ Hz, $(\text{CH}_3)_2\text{CH}-7$), 2.53 (3H, s, Me-1), 2.70 (1H, sept, $J=6.9$ Hz, $(\text{CH}_3)_2\text{CH}-7$), 2.93 (3H, s, Me-4), 6.74 (1H, d, $J=10.8$ Hz, H-5), 7.12 (1H, dd, $J=10.8, 2.2$ Hz, H-6), 8.05 (1H, br s, H-2), and 8.09 (1H, d, $J=2.2$ Hz, H-8); signals based on a 4-(dimethylamino)phenyl group: δ 2.42 (6H, s, $(\text{CH}_3)_2\text{N}-4''$), 6.51 (2H, dd, $J=8.8, 2.6$ Hz, H-3'',5''), and 7.33 (2H, dd, $J=8.8, 2.6$ Hz, H-2'',6''); and signals based on a *cis*-3,6-substituted 1,1,2,2-tetracyano-4-cyclohexene unit: δ 4.11 (1H, ddd, $J=2.8, 2.8, 2.8$ Hz, H-3'), 5.64 (1H, ddd, $J=10.6, 3.0, 2.8$ Hz, H-4'), 5.66 (1H, ddd, $J=3.0, 2.8, 2.8$ Hz, H-6'), and 5.84 (1H, ddd, $J=10.6, 3.0, 2.8$ Hz, H-5'); 176 MHz ^{13}C NMR (benzene- d_6), δ 151.4 (C-4''), 144.4 (C-4), 142.2 (C-7), 140.7 (C-2), 140.2 (C-8a), 135.6 (C-6), 135.1 (C-8,3a), 131.5 (C-2'',6''), 130.2 (C-5), 128.3 (C-5'), 125.9 (C-4'), 125.0 (C-1), 120.1 (C-1''), 117.0 (C-3), 113.3, 112.6, 111.0, 110.7 (CN each), 112.2 (C-3'',5''), 46.6 (C-3'), 45.0, 44.7 (C-1',2'), 42.7 (C-6'), 39.6 ($(\text{CH}_3)_2\text{N}-4''$), 37.8 ($(\text{CH}_3)_2\text{CH}-7$), 28.1 (Me-4), 24.4 ($(\text{CH}_3)_2\text{CH}-7$), and 13.0 (Me-1).

4.1.5. X-ray crystal structure of 3-{1,1,2,2-tetracyano-*cis*-3-[4-(dimethylamino)phenyl]-4-cyclohexen-6-yl}guaiazulene (8) with an equivalent of AcOEt molecule. A total 7779 reflections with $2\theta_{\text{max}}=55.0^\circ$ were collected on a Rigaku AFC-5R automated four-circle diffractometer with graphite monochromated Mo $K\alpha$ radiation ($\lambda=0.71069$ Å, rotating anode: 50 kV, 180 mA) at -75 °C. The structure was solved by direct methods (SIR97) and expanded using Fourier techniques (DIRDIF94). Non-hydrogen atoms were refined anisotropically. Hydrogen atoms were included but not refined. The final cycle of full-matrix least-squares refinement was based on F^2 . All calculations were performed using the teXsan crystallographic software package. Deposition number CCDC-669772 for compound No. **8**.

Crystallographic data for **8** with an equivalent of AcOEt molecule: $\text{C}_{37}\text{H}_{39}\text{O}_2\text{N}_5$ (FW=585.75), blue plate (crystal size, $0.50 \times 0.40 \times 0.90$ mm 3), triclinic, $P-1$ (#2), $a=14.174(4)$ Å, $b=15.123(4)$ Å, $c=8.005(5)$ Å, $\alpha=94.53(4)^\circ$, $\beta=100.11(4)^\circ$, $\gamma=74.27(2)^\circ$, $V=1625(1)$ Å 3 , $Z=2$, $D_{\text{calcd}}=1.197$ g/cm 3 , $\mu(\text{Mo } K\alpha)=0.75$ cm $^{-1}$, scan width= $(1.37+0.30 \tan\theta)^\circ$, scan mode= $\omega-2\theta$, scan rate= $14.0^\circ/\text{min}$, measured reflections=7779, observed reflections=7476, No. of parameters=397, $R1=0.067$, $wR2=0.183$, goodness of fit indicator=1.49.

4.1.6. Reaction of (2E,4E)-4-[4-(dimethylamino)phenyl]-1-(3-guaiazulenyl)-1,3-butadiene (6E) with (E)-1,2-dicyanoethylene (DCNE). To a solution of compound **6E** (15 mg, 41 μmol) in *p*-xylene (2 mL) was added a solution of DCNE (7 mg, 90 μmol) in *p*-xylene (2 mL) under argon. The mixture was stirred at reflux temperature (138 °C) for

four days under argon. After the reaction, the reaction solution was evaporated in vacuo. The residue thus obtained was carefully separated by silica gel column chromatography with hexane/ethyl acetate (3:1, vol/vol) as an eluant. The crude product was recrystallized from hexane/ethyl acetate (5:1, vol/vol) (several times) to provide pure 3-{1,2-dicyano-3-[4-(dimethylamino)phenyl]-4-cyclohexen-6-yl}guaiazulene (**9**) (10 mg, 22 μmol , 54% yield) as stable crystals.

Compound 9: Blue needles [$R_f=0.25$ on silica gel TLC (solvent: hexane/ethyl acetate=3:1, vol/vol)]; mp 259 °C; UV-vis $\lambda_{\text{max}}/\text{nm}$ (log ϵ) in benzene, 295 (4.80), 307sh (4.58), 353 (3.90), 370 (3.87), 609 (2.78), 666sh (2.68), and 738sh (2.21); IR $\nu_{\text{max}}/\text{cm}^{-1}$ (KBr), 3024–2808 (C–H), 2245 (C \equiv N), 1612, 1524 (C=C), and 1362 (C–N); exact FABMS (3-nitrobenzyl alcohol matrix), found: m/z 447.2692; calcd for $\text{C}_{31}\text{H}_{33}\text{N}_3$: M^+ , m/z 447.2674. The relative intensity of the ^1H NMR signals for the diastereomers **9a** and **9b** showed a ratio of ca. 5:3.

Compound 9a: 700 MHz ^1H NMR (benzene- d_6), signals based on a 3-guaiazulenyl group: δ 1.19 (6H, d, $J=7.0$ Hz, $(\text{CH}_3)_2\text{CH}-7$), 2.52 (3H, s, Me-1), 2.78 (1H, sept, $J=7.0$ Hz, $(\text{CH}_3)_2\text{CH}-7$), 2.91 (3H, s, Me-4), 6.83 (1H, d, $J=10.6$ Hz, H-5), 7.17 (1H, dd, $J=10.6, 2.2$ Hz, H-6), 7.72 (1H, s, H-2), and 8.17 (1H, d, $J=2.2$ Hz, H-8); signals based on a 4-(dimethylamino)phenyl group: δ 2.54 (6H, s, $(\text{CH}_3)_2\text{N}-4''$), 6.64 (2H, dd, $J=8.6, 2.5$ Hz, H-3'',5''), and 7.32 (2H, dd, $J=8.6, 2.5$ Hz, H-2'',6''); and signals based on a 1,2-dicyano-4-cyclohexene unit possessing two substituents at the C-3 and C-6 positions: δ 2.60 (1H, dd, $J=10.6, 5.8$ Hz, H-1'), 3.04 (1H, dd, $J=10.6, 9.5$ Hz, H-2'), 3.37 (1H, dddd, $J=9.5, 2.3, 2.2, 2.2$ Hz, H-3'), 4.73 (1H, dddd, $J=5.8, 4.2, 2.4, 2.2$ Hz, H-6'), 5.67 (1H, ddd, $J=9.9, 2.4, 2.2$ Hz, H-4'), and 5.71 (1H, ddd, $J=9.9, 4.2, 2.4$ Hz, H-5'); 176 MHz ^{13}C NMR (benzene- d_6), δ 150.6 (C-4''), 140.6 (C-4,7), 139.6 (C-8a), 139.4 (C-2), 135.4 (C-6), 134.5 (C-8), 134.2 (C-3a), 131.2 (C-4'), 129.0 (C-5',2'',6''), 128.8 (C-5), 125.0 (C-1), 124.6 (C-1''), 122.6 (CN), 119.2 (CN), 117.6 (C-3), 113.2 (C-3'',5''), 44.4 (C-3') 40.0 ($(\text{CH}_3)_2\text{N}-4''$), 37.8 ($(\text{CH}_3)_2\text{CH}-7$), 35.9 (C-1'), 35.3 (C-6'), 34.2 (C-2'), 28.5 (Me-4), 24.6 ($(\text{CH}_3)_2\text{CH}-7$), and 13.2 (Me-1).

Compound 9b: 700 MHz ^1H NMR (benzene- d_6), signals based on a 3-guaiazulenyl group: δ 1.22 (6H, d, $J=7.0$ Hz, $(\text{CH}_3)_2\text{CH}-7$), 2.52 (3H, s, Me-1), 2.79 (1H, sept, $J=7.0$ Hz, $(\text{CH}_3)_2\text{CH}-7$), 2.90 (3H, s, Me-4), 6.75 (1H, d, $J=10.6$ Hz, H-5), 7.15 (1H, dd, $J=10.6, 2.0$ Hz, H-6), 7.59 (1H, s, H-2), and 8.14 (1H, d, $J=2.0$ Hz, H-8); signals based on a 4-(dimethylamino)phenyl group: δ 2.54 (6H, s, $(\text{CH}_3)_2\text{N}-4''$), 6.64 (2H, dd, $J=8.6, 2.5$ Hz, H-3'',5''), and 7.34 (2H, dd, $J=8.6, 2.5$ Hz, H-2'',6''); and signals based on a 1,2-dicyano-4-cyclohexene unit possessing two substituents at the C-3 and C-6 positions: δ 2.57 (1H, dd, $J=11.2, 5.2$ Hz, H-2'), 3.13 (1H, dd, $J=11.2, 10.0$ Hz, H-1'), 3.31 (1H, dddd, $J=5.2, 4.8, 2.2, 2.0$ Hz, H-3'), 4.67 (1H, dddd, $J=10.0, 2.2, 2.2, 2.2$ Hz, H-6'), 5.37 (1H, ddd, $J=10.0, 4.8, 2.2$ Hz, H-4'), and 5.67 (1H, ddd, $J=10.0, 2.2, 2.0$ Hz, H-5'); 176 MHz ^{13}C NMR (benzene- d_6), δ 150.7 (C-4''), 140.5 (C-4,7), 139.6 (C-8a), 136.9 (C-2), 135.0 (C-6), 134.3 (C-8), 133.2 (C-3a), 130.8 (C-2'',6''), 128.8 (C-5), 128.3 (C-5'), 125.5 (C-4'), 125.0 (C-1), 124.5 (C-1''), 122.6 (CN), 119.2 (CN), 117.8 (C-3), 112.7 (C-3'',5''), 40.6 (C-3'), 40.2 (C-6'), 40.1 ($(\text{CH}_3)_2\text{N}-4''$), 37.9 ($(\text{CH}_3)_2\text{CH}-7$), 36.3 (C-2'), 33.9 (C-1'), 28.1 (Me-4), 24.5 ($(\text{CH}_3)_2\text{CH}-7$), and 13.3 (Me-1).

4.1.7. Reaction of (2E,4E)-4-[4-(dimethylamino)phenyl]-1-(3-guaiazulenyl)-1,3-butadiene (6E) with dimethyl acetylenedicarboxylate (DMAD). To a solution of compound **6E** (31 mg, 84 μmol) in toluene (5 mL) was added a solution of DMAD (40 μL , 326 μmol) under argon. The mixture was stirred at reflux temperature (110 °C) for two days under argon. After the reaction, the reaction solution was evaporated in vacuo. The residue thus obtained was carefully separated by silica gel column chromatography with hexane/ethyl acetate (2:1, vol/vol) as an eluant. The crude product thus obtained was recrystallized from hexane/ethyl acetate (5:1, vol/vol) to

provide pure 3-[1,2-dimethoxycarbonyl-*cis*-3-[4-(dimethylamino)phenyl]-1,4-cyclohexadiene-6-yl]guaiazulene (**10**) (25 mg, 49 μmol , 58% yield) as a solid.

Compound 10: Blue solid [R_f]=0.35 on silica gel TLC (solvent, hexane/ethyl acetate=2:1, vol/vol); UV-vis λ_{max} /nm (log ϵ) in benzene, 294 (4.66), 309sh (4.47), 358 (3.93), 376 (3.91), 616 (2.73), 670sh (2.65), and 750sh (2.27); exact FABMS (3-nitrobenzyl alcohol matrix), found: m/z 511.2723; calcd for $\text{C}_{33}\text{H}_{37}\text{O}_4\text{N}$: M^+ , m/z 511.2723; 700 MHz ^1H NMR (benzene- d_6), signals based on a 3-guaiazulenyl group: δ 1.189, 1.190 (3H each, d, $J=7.0$ Hz, $(\text{CH}_3)_2\text{CH}-7$), 2.49 (3H, br s, Me-1), 2.76 (1H, sept, $J=7.0$ Hz, $(\text{CH}_3)_2\text{CH}-7$), 2.93 (3H, br s, Me-4), 6.73 (1H, d, $J=10.6$ Hz, H-5), 7.12 (1H, dd, $J=10.6, 2.2$ Hz, H-6), 8.08 (1H, d, $J=2.2$ Hz, H-8), and 8.08 (1H, br s, H-2); signals based on a 4-(dimethylamino)phenyl group: δ 2.52 (6H, s, $(\text{CH}_3)_2\text{N}-4''$), 6.67 (2H, dd, $J=8.6, 2.5$ Hz, H-3'',5''), and 7.46 (2H, dd, $J=8.6, 2.5$ Hz, H-2'',6''); and signals based on a *cis*-3,6-di-substituted 1,2-dimethoxycarbonyl-1,4-cyclohexadiene unit: δ 3.08, 3.40 (3H each, s, $\text{H}_3\text{COOC}-1$ or 2), 4.62 (1H, m, H-3'), 5.63, 5.64 (1H each, m, H-5', 6'), and 5.84 (1H, m, H-4'); 176 MHz ^{13}C NMR (benzene- d_6), δ 168.9, 167.8 ($\text{H}_3\text{COOC}-1'$ or 2'), 150.1 (C-4''), 144.8 (C-4), 139.8 (C-8a), 139.6 (C-7), 139.4 (C-2), 138.2 (C-2'), 134.4 (C-6), 134.3 (C-1'), 133.8 (C-8), 131.9 (C-3a), 129.8 (C-2'',6''), 129.5 (C-1''), 127.9 (C-4'), 127.2 (C-5), 125.4 (C-1), 124.5 (C-5'), 113.1 (C-3'',5''), 51.5, 51.4 ($\text{H}_3\text{COOC}-1'$ or 2'), 44.0 (C-3'), 40.2 ($(\text{CH}_3)_2\text{N}-4''$), 38.2 (C-6'), 37.9 ($(\text{CH}_3)_2\text{CH}-7$), 27.4 (Me-4), 24.63, 24.60 ($(\text{CH}_3)_2\text{CH}-7$), and 13.2 (Me-1). The C-3 carbon signal was included in other signals.

4.1.8. Oxidation of 3-[1,2-dimethoxycarbonyl-*cis*-3-[4-(dimethylamino)phenyl]-1,4-cyclohexadiene-6-yl]guaiazulene (10**) with MnO_2 .** To a solution of compound **10** (25 mg, 49 μmol) in dichloromethane (5 mL) was added a solution of dichloromethane (5 mL) with MnO_2 (10 mg, 115 μmol). The mixture was stirred at 25 $^\circ\text{C}$ for 24 h. After the reaction, MnO_2 was removed by using a centrifugal separator and then the reaction solution was evaporated in vacuo. The residue thus obtained was carefully separated by silica gel column chromatography with hexane/ethyl acetate (2:1, vol/vol) as an eluant. The crude product thus obtained was recrystallized from hexane/ethyl acetate (5:1, vol/vol) to provide pure 3-[1,2-dimethoxycarbonyl-*cis*-3-[4-(methylamino)phenyl]-1,4-cyclohexadiene-6-yl]guaiazulene (**11**) (9 mg, 18 μmol , 37% yield) as stable crystals.

Compound 11: Blue blocks [R_f]=0.25 on silica gel TLC (solvent, hexane/ethyl acetate=2:1, vol/vol); mp 181 $^\circ\text{C}$; exact FABMS (3-nitrobenzyl alcohol matrix), found: m/z 497.2551; calcd for $\text{C}_{32}\text{H}_{35}\text{O}_4\text{N}$: M^+ , m/z 497.2566; 700 MHz ^1H NMR (benzene- d_6), signals based on a 3-guaiazulenyl group: δ 1.190, 1.191 (3H each, d, $J=7.0$ Hz, $(\text{CH}_3)_2\text{CH}-7$), 2.48 (3H, br s, Me-1), 2.76 (1H, sept, $J=7.0$ Hz, $(\text{CH}_3)_2\text{CH}-7$), 2.92 (3H, br s, Me-4), 6.72 (1H, d, $J=10.6$ Hz, H-5), 7.12 (1H, dd, $J=10.6, 2.0$ Hz, H-6), 8.06 (1H, br s, H-2), and 8.08 (1H, d, $J=2.0$ Hz, H-8); signals based on a 4-(methylamino)phenyl group: δ 2.32 (3H, s, $\text{CH}_3\text{NH}-4''$), 6.44 (2H, dd, $J=8.4, 2.3$ Hz, H-3'',5''), and 7.39 (2H, dd, $J=8.4, 2.3$ Hz, H-2'',6''). The $\text{MeNH}-4''$ proton signal was not observed; and signals based on a *cis*-3,6-disubstituted 1,2-dimethoxycarbonyl-1,4-cyclohexadiene unit: δ 3.08, 3.40 (3H each, s, $\text{H}_3\text{COOC}-1$ or 2), 4.59 (1H, m, H-3'), 5.61, 5.62 (1H each, m, H-5', 6'), and 5.83 (1H, m, H-4'); 176 MHz ^{13}C NMR (benzene- d_6), δ 169.0, 167.7 ($\text{H}_3\text{COOC}-1'$ or 2'), 148.9 (C-4''), 144.8 (C-4), 139.7 (C-8a), 139.6 (C-7), 139.4 (C-2), 138.5 (C-2'), 134.4 (C-6), 134.1 (C-1'), 133.7 (C-8), 131.9 (C-3a), 129.9 (C-2'',6''), 128.3 (C-4'), 127.2 (C-5), 125.3 (C-1), 124.5 (C-5'), 112.7 (C-3'',5''), 51.5, 51.4 ($\text{H}_3\text{COOC}-1'$ or 2'), 44.2 (C-3'), 38.1 (C-6'), 37.9 ($(\text{CH}_3)_2\text{CH}-7$), 30.4 ($\text{CH}_3\text{NH}-4''$), 27.3 (Me-4), 24.62, 24.60 ($(\text{CH}_3)_2\text{CH}-7$), and 13.1 (Me-1). The C-3 and C-1'' carbon signals were included in other signals.

4.1.9. X-ray crystal structure of 3-[1,2-dimethoxycarbonyl-*cis*-3-[4-(methylamino)phenyl]-1,4-cyclohexadiene-6-yl]guaiazulene (11**).** The

X-ray measurement of the single crystal **11** was made on a Rigaku Saturn CCD area detector with graphite monochromated Mo $K\alpha$ radiation ($\lambda=0.71075$ \AA) at -140 ± 1 $^\circ\text{C}$. The structure was solved by direct methods (SIR92) and expanded using Fourier techniques (DIRDIF99). Non-hydrogen atoms were refined anisotropically. Hydrogen atoms were included but not refined. The final cycle of full-matrix least-squares refinement was based on F^2 . All calculations were performed using the Crystal Structure crystallographic software package developed by Rigaku corporation, Japan. Deposition number CCDC-749884 for compound No. **11**.

Crystallographic data for **11**: $\text{C}_{32}\text{H}_{35}\text{O}_4\text{N}$ (FW=497.63), blue block (the crystal size, $0.64\times 0.35\times 0.10$ mm^3), monoclinic, $P2_1/n$ (#14), $a=12.444(3)$ \AA , $b=10.355(2)$ \AA , $c=20.602(4)$ \AA , $\beta=93.547(5)^\circ$, $V=2649.7(9)$ \AA^3 , $Z=4$, $D_{\text{calcd}}=1.247$ g/cm^3 , $\mu(\text{Mo } K\alpha)=0.813$ cm^{-1} , measured reflections=25,169, observed reflections=3747, No. of parameters=370, $R1=0.0674$, $wR2=0.1997$, goodness of fit indicator=0.964.

Acknowledgements

This work was partially supported by a Grant-in-Aid for Scientific Research from the Ministry of Education, Culture, Sports, Science, and Technology, Japan.

Supplementary data

Supplementary data associated with this article can be found in the online version, at doi:10.1016/j.tet.2010.02.064.

References and notes

- Takekuma, S.; Sasaki, M.; Takekuma, H.; Yamamoto, H. *Chem. Lett.* **1999**, 999–1000.
- Takekuma, S.; Takata, S.; Sasaki, M.; Takekuma, H. *Tetrahedron Lett.* **2001**, 42, 5921–5924.
- Takekuma, S.; Tanizawa, M.; Sasaki, M.; Matsumoto, T.; Takekuma, H. *Tetrahedron Lett.* **2002**, 43, 2073–2078.
- Sasaki, M.; Nakamura, M.; Hannita, G.; Takekuma, H.; Minematsu, T.; Yoshihara, M.; Takekuma, S. *Tetrahedron Lett.* **2003**, 44, 275–279.
- Sasaki, M.; Nakamura, M.; Uriu, T.; Takekuma, H.; Minematsu, T.; Yoshihara, M.; Takekuma, S. *Tetrahedron* **2003**, 59, 505–516.
- Nakamura, M.; Sasaki, M.; Takekuma, H.; Minematsu, T.; Takekuma, S. *Bull. Chem. Soc. Jpn.* **2003**, 76, 2051–2052.
- Takekuma, S.; Sasaki, K.; Nakatsuji, M.; Sasaki, M.; Minematsu, T.; Takekuma, H. *Bull. Chem. Soc. Jpn.* **2004**, 77, 379–380.
- Nakatsuji, M.; Hata, Y.; Fujihara, T.; Yamamoto, K.; Sasaki, M.; Takekuma, H.; Yoshihara, M.; Minematsu, T.; Takekuma, S. *Tetrahedron* **2004**, 60, 5983–6000.
- Takekuma, S.; Hata, Y.; Nishimoto, T.; Nomura, E.; Sasaki, M.; Minematsu, T.; Takekuma, H. *Tetrahedron* **2005**, 61, 6892–6907.
- Takekuma, S.; Takahashi, K.; Sakaguchi, A.; Shibata, Y.; Sasaki, M.; Minematsu, T.; Takekuma, H. *Tetrahedron* **2005**, 61, 10349–10362.
- Takekuma, S.; Takahashi, K.; Sakaguchi, A.; Sasaki, M.; Minematsu, T.; Takekuma, H. *Tetrahedron* **2006**, 62, 1520–1526.
- Takekuma, S.; Hirose, M.; Morishita, S.; Sasaki, M.; Minematsu, T.; Takekuma, H. *Tetrahedron* **2006**, 62, 3732–3738.
- Takekuma, S.; Sonoda, K.; Fukuhara, C.; Minematsu, T. *Tetrahedron* **2007**, 63, 2472–2481.
- Takekuma, S.; Tone, K.; Sasaki, M.; Minematsu, T.; Takekuma, H. *Tetrahedron* **2007**, 63, 2490–2502.
- Takekuma, S.; Mizutani, K.; Inoue, K.; Nakamura, M.; Sasaki, M.; Minematsu, T.; Sugimoto, K.; Takekuma, H. *Tetrahedron* **2007**, 63, 3882–3893.
- Takekuma, S.; Tamura, M.; Minematsu, T.; Takekuma, H. *Tetrahedron* **2007**, 63, 12058–12070.
- Takekuma, S.; Sonoda, K.; Minematsu, T.; Takekuma, H. *Tetrahedron* **2008**, 64, 3802–3812.
- Takekuma, S.; Hori, S.; Minematsu, T.; Takekuma, H. *Bull. Chem. Soc. Jpn.* **2008**, 81, 1472–1484.
- Takekuma, S.; Hori, S.; Minematsu, T.; Takekuma, H. Article ID 684359, 5 pages (open access article) *Res. Lett. Org. Chem.* **2009**. doi:10.1155/2009/684359
- Takekuma, S.; Ijibata, N.; Minematsu, T.; Takekuma, H. *Bull. Chem. Soc. Jpn.* **2009**, 82, 585–593.
- Takekuma, S.; Fukuda, K.; Kawase, Y.; Minematsu, T.; Takekuma, H. *Bull. Chem. Soc. Jpn.* **2009**, 82, 879–890.
- Takekuma, S.; Fukuda, K.; Minematsu, T.; Takekuma, H. *Bull. Chem. Soc. Jpn.* **2009**, 82, 1398–1408.

23. Shoji, T.; Ito, S.; Okujima, T.; Higashi, J.; Yokoyama, R.; Toyota, K.; Yasunami, M.; Morita, N. *Eur. J. Org. Chem.* **2009**, 1554–1563.
24. Asato, A. E.; Peng, A.; Hossain, M. Z.; Mirzadegan, T.; Bertram, J. S. *J. Med. Chem.* **1993**, 36, 3137–3147.
25. Gage, J. L.; Kirst, H. A.; O'Neil, D.; David, B. A.; Smith, C. K., II; Naylor, S. A. *Bioorg. Med. Chem.* **2003**, 11, 4083–4091.
26. Tessore, F.; Roberto, D.; Ugo, R.; Pizzotti, M. *Inorg. Chem.* **2005**, 44, 8967–8978.
27. Coe, B. J.; Harris, J. A.; Hall, J. J.; Brunshwig, B. S.; Hung, S.-T.; Libaers, W.; Clays, K.; Coles, S. J.; Horton, P. N.; Light, M. E.; Hursthouse, M. B.; Garín, J.; Orduna, J. *Chem. Mater.* **2006**, 18, 5907–5918.
28. Liu, Z.; Fang, Q.; Wang, D.; Cao, D.; Xue, G.; Yu, W.; Lei, H. *Chem.—Eur. J.* **2003**, 9, 5074–5084.
29. Davis, R.; Abraham, S.; Rath, N. P.; Das, S. *New J. Chem.* **2004**, 28, 1368–1372.
30. Rodriguez, J. G.; Tejedor, J. L.; Rumbero, A.; Canoira, L. *Tetrahedron* **2006**, 62, 3075–3080.
31. Dumur, F.; Mayer, C. R.; Dumas, E.; Miomandre, F.; Frigoli, M.; Sécheresse, F. *Org. Lett.* **2008**, 10, 321–324.
32. (2*Z*,4*E*)-4-[4-(Dimethylamino)phenyl]-1-(3-guaiazulenyl)-1,3-butadiene (**6Z**): Green paste [*R_f*=0.26 on silica gel TLC (solv. hexane/ethyl acetate=9:1, vol/vol) under the same conditions as for **6E**]; 500 MHz ¹H NMR (benzene-*d*₆), signals based on a 3-guaiazulenyl group: δ 1.20 (6H, d, *J*=7.0 Hz, (CH₃)₂CH-7'), 2.54 (3H, br s, Me-1'), 2.76 (1H, sept, *J*=7.0 Hz, (CH₃)₂C H-7'), 2.86 (3H, s, Me-4'), 6.64 (1H, *J*=10.6 Hz, H-5'), 7.07 (1H, dd, *J*=10.6, 2.0 Hz, H-6'), 7.97 (1H, br s, H-2'), and 8.07 (1H, d, *J*=2.0 Hz, H-8'); signals based on a 4-(dimethylamino)phenyl group: δ 2.44 (6H, s, (CH₃)₂N-4''), 6.43 (2H, dd, *J*=8.8, 2.3 Hz, H-3'',5''), and 7.33 (2H, dd, *J*=8.8, 2.3 Hz, H-2'',6''); and signals based on a (2*Z*,4*E*)-1,3-butadiene unit: δ 6.59 (1H, ddd, *J*=11.2, 10.8, 0.6 Hz, H-2), 6.85 (1H, br d, *J*=15.4 Hz, H-4), 7.21 (1H, br d, *J*=10.8 Hz, H-1), and 7.63 (1H, ddd, *J*=15.4, 11.2, 1.2 Hz, H-3).
33. The accurate parameters for the crystal structures of **6E^B** and **12** were transferred to a WinMOPAC (Ver. 3.0) program³⁴ and their dipole moments and π-HOMO–π-LUMO energy levels were calculated. A keyword (1 SCF) was used.
34. The computer program was developed by Fujitsu Ltd., Japan.
35. Careful study of the ¹H NMR signals suggested a 1:1, mixture of **8** and AcOEt and further, a molecule of **8** with an equivalent of AcOEt molecule was found to exist in the unit cell of the crystal by means of X-ray crystallographic analysis.
36. Guaiazulene (**1**): UV–vis λ_{max}/nm (log ε) in CH₃CN, 213 (4.10), 244 (4.39), 284 (4.61), 301sh (4.03), 348 (3.65), 365 (3.46), 600(2.68), 648sh (2.61), and 721sh (2.20).
37. O'Shea, K. E.; Foote, C. S. *Tetrahedron Lett.* **1990**, 31, 841–844.
38. Matsubara, Y.; Yamamoto, H.; Nozoe, T. Studies in natural products chemistry. In *Stereoselective Synthesis (Part I)*; Rahman, Atta-ur-, Ed.; Elsevier: Amsterdam, 1994; Vol. 14, pp 313–354.
39. Moreau, P.; Guillaumont, G.; Coudert, G. *Tetrahedron* **1994**, 50, 3407–3414.